THE JOURNAL OF PHYSICAL CHEMISTRY C

Article

pubs.acs.org/JPCC

The Role of Passivants on the Stoichiometry of CdSe and GaAs Nanocrystals

Saikat Debnath, Roby Cherian,[†] and Priya Mahadevan*

Department of Condensed Matter Physics and Material Sciences, S. N. Bose National Centre for Basic Sciences, Block: JD, Sector III, Salt Lake, Kolkata-700098, India

ABSTRACT: Passivating molecules are introduced during the growth of semiconductor nanocrystals (NCs) to arrest their growth leading to nanoparticles of a desired size. In order to carry out this function, they bind to the surface atoms of the NC, removing any band gap states in the process. While they have been observed to play a role in modifying various other physical properties of materials, in this work we consider examples of two well-known binary semiconductors, GaAs and CdSe, and find within our calculations that the passivating ligands can play an important role in stabilizing highly nonstoichiometric semiconductors. This has important implications in the observed optical and electronic properties of binary semiconductor NCs where usually no suitable passivant exists for the anion.

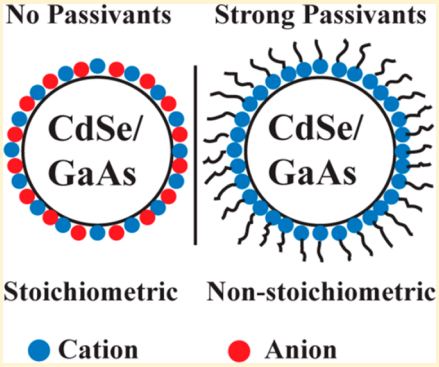

INTRODUCTION

One finds significantly different properties from the bulk as one approaches the nano regime. This has led to intense research activity in these materials over the past two decades. The strong dependence of physical properties on size, found especially in semiconductors, has significant technological implications, and this coupled with the ease of fabrication and processing makes this class of materials promising building blocks for materials with designed functions.[1−3] In the past decade or so, the colloidal chemistry route to the synthesis of nano particles has emerged as a popular route to semiconductor nano particles with wide-ranging applications.[4−7] Access to a control of the properties requires an ability to control the uniformity of size, shape, composition, crystal structure, surface, magnetic, optical, and other properties. Theoretically various aspects of the physics of NCs have been investigated in the past using ab initio methods, which have been quite successful in explaining various experimentally observed phenomena. The self-purification of dopants in Si NCs,[8] Mn emission in Mn-doped CdS NCs,[9] magnetic properties of Fe/Cu-codoped ZnO NCs,[10] and role of dimensionality and quantum confinement in p-type semiconductor indium phosphide quantum dots (QDs)[11] are some examples that have been successfully investigated.

A typical synthesis of nanoparticles consists of three components: precursors, surfactants, and solvent(s). Initially the precursors decompose in solution or react at relatively high temperatures to form a supersaturation of monomers/dimers/trimers etc. followed by a burst of nucleation centers and the growth of nanoparticles. A passivant that is usually an organic surfactant is used to prevent an uncontrolled agglomeration of nanoparticles. These organic molecules attach themselves to the surface of the NCs and prevent agglomeration by means of charge neutralization. They also saturate all surface dangling bonds to prevent any optical transitions involving surface states.[12,13]

The role of the introduced passivants has been seen to be more than a parameter introduced during the growth of the nanoparticles to control the size of the NC. Earlier works have found them responsible for nontraditional roles,[14−17] which emerge as a consequence of their binding with the surface atoms. In the case of thiolated gold nanoparticles,[18] what has been seen is that the strong interaction between the ligand atoms of the passivant and the gold atoms changes the d electron count of the surface atoms, thus inducing a small magnetic moment. The early work by Peng et al.[19] showed that some of the ligands were found to bind more strongly than others to the cations on the surface. As different surfaces had different number of cations, this led to the growth of highly anisotropic structures with those directions to which fewer passivants were attached growing faster than others. This interaction could also in some cases modify the bandgap of the semiconductor.[20] This is because in the ideal case, the passivant would interact with the surface atoms and remove band gap states. However, in the case that the interactions were not strong enough, the states would remain in the band gap region, thereby determining the band gap.[20] The oscillator strengths for the optical transitions associated with such transitions would be drastically reduced compared to the band edge transitions involving atoms from the core region of the NC.[21,22]

Binary semiconductors that belong to III−V and II−VI groups of the periodic table mainly exist in two different phases, wurtzite and zincblende, with the energy difference between

Received: February 20, 2013
Revised: September 21, 2013
Published: September 23, 2013

 © 2013 American Chemical Society

them being very small, on the order of a few millielectronvolts.[23] It has been shown that the choice of the passivant as a result of stronger binding to a particular surface could induce a change in the delicate energy balance that determines the favored crystal structure[14,15] in these systems.

Thus the strong interaction of the ligand has been recognized to lead to modifications of the properties of the NC compared to their bulk counterparts. In this work, we go a step further in this direction. Considering a cation at the surface, when confronted with the choice of binding to a passivating ligand and an anion, one finds that it is the strength of the bond that dictates the choice. Atoms at different surfaces, however, have different coordinations with the atoms of the layer below. A stronger binding with the passivating ligand implies that those surfaces in which the surface atoms form more bonds with the passivating ligands are the ones that are stabilized. Analyzing a few surfaces in the case of zincblende semiconductors, we find that the polar surfaces are the more undercoordinated surfaces. As a result, considering the example of CdSe and GaAs, enroute to the bulk limit, we find that the passivating ligands play an important role in controlling the surface stoichiometry and could in turn result in the growth of highly nonstoichiometric NCs.

COMPUTATIONAL METHOD

NCs of GaAs and CdSe were generated preserving the underlying tetrahedral coordination of the bulk zincblende lattice. In one scheme of generation, NCs were generated by considering a central atom and adding one layer at a time. The structure generated for GaAs for the case where four layers were added ($l = 4$) is shown in Figure 1a. This is generated by considering a Ga atom at the core. The first layer ($l = 1$) that is added consists of four As atoms, which are singly coordinated with the Ga atom at the core. The next layer ($l = 2$) of 12 Ga atoms are then added and depending on the number of layers, l subsequent layers are added. This scheme of generation led to highly nonstoichiometric NCs as we can see from Table 1. While we considered the central atom to be Ga in the case of GaAs, it was taken to be Se in the case of CdSe NCs. In the other scheme of generation of the NCs, spheres of desired radii centered at an atom were cut out from supercells of the zincblende structure. These are shown in Figure 1b, and the generated NCs are almost stoichiometric as one finds in Table 1. In the present case, the label l is used to denote the maximum number of layers present in the NC. While we took these NCs as the starting structures for a set of calculations, the surface atoms were passivated with cationic (passivant that attaches to the anion) and anionic (passivant that attaches to the cation) pseudohydrogens with the proper charge to neutralize the charge on the atom[24] for another set of calculations. For instance, considering the example of CdSe, each Cd atom donates 0.5 electron to each CdSe bond. So, a passivant that attaches itself to Cd should have the charge 1.5, so that it has a filled shell after receiving the charge from Cd. Similarly, the cationic passivant that attaches itself to Se has a charge of 0.5, so that it has an empty shell after donating the charge to Se. In the case of GaAs, we have used cationic and anionic passivants of charges 0.25e and 1.75e respectively. For a single coordinated (coordination between Ga and As or Cd and Se) surface atom we have used three such passivants, for double coordinated surface atom two such passivants have been used and for triple coordinated atom, one such passivant has been used (Figure 1). This methodology has been used extensively and successfully in the literature to explain various effects.[9,10,25−27]

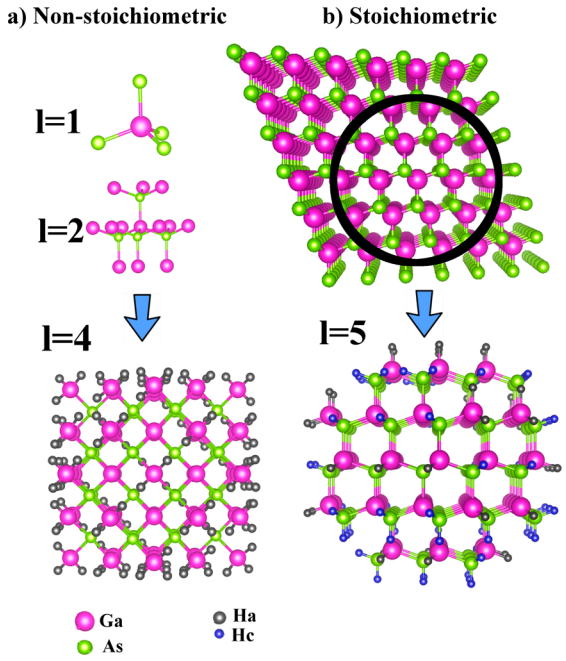

Figure 1. Structure generation procedure for nonstoichiometric and stoichiometric passivated structures of GaAs NCs. (a) Nonstoichiometric structures were generated by adding concentric layers of cations and anions. (b) Stoichiometric structures were generated by truncating spheres from supercell.

As the implementation of density functional theory that we use is for periodic systems, 12 Å of vacuum is introduced in each direction to minimize the interactions between periodic images. Electronic structure calculations were performed within a plane wave pseudo potential implementation of density functional theory as implemented in the Vienna Ab initio Simulation Package code (VASP)[28,29] using projector augmented wave (PAW)[30] potentials. The potential used for Ga had the Ga d states as a part of the core as this was seen to be adequate earlier.[31] The GGA PW91[32] approximation for the exchange correlation functional has been used. All calculations were performed at gamma point alone. Full geometrical relaxations were done for all structures until an energy convergence better than 10^{-5} eV was achieved and the atomic force on each atom was less than 5 meV/Å. A flowchart of the calculations is shown in Figure 2. Volume of the relaxed NCs was determined by the convex hull method, and radii have been calculated by mapping volume into the formula of a sphere.

For the surface calculations we have chosen the non polar (110) as well as the polar (100), (111) surfaces for the zincblende structure. Slabs consisting of 16 CdSe monolayers were used to mimic the (110) surface while we used 17 CdSe monolayers to mimic (100) and (111) Se surfaces. Vacuum of 12 Å between two periodic images along the growth direction was introduced to minimize the interaction between images. A gamma centered 6 × 6 × 1 K points mesh was used for the surface calculations. The surface calculations were performed with pseudo hydrogen with the appropriate charge as used in the case of the NCs. These results were contrasted with those in which no passivant was used.

dx.doi.org/10.1021/jp401798y | J. Phys. Chem. C 2013, 117, 21981−21987

Table 1. Structural Formula, Approximate Radii, Number of Atoms with Different Coordinations, and Fraction of Single and Double Coordinated Atoms in 'A' Centered Binary NCs of Type A_mB_n as a Function of the Number of Layers 'l'

		radii in Å		number of atoms with coordination				
nonstoichiometric	structural formula	GaAs	CdSe	1	2	3	4	% of single and double coordinated atoms
l = 1	A_1B_4	2.5	2.7	4(B)	-	-	1(A)	80
l = 2	$A_{13}B_4$	4.3	4.5	12(A)	-	-	1(A),4(B)	71
l = 3	$A_{13}B_{28}$	6.0	6.7	12(B)	12(B)	-	13(A),4(B)	59
l = 4	$A_{55}B_{28}$	8.0	8.3	24(A)	18(A)	-	13(A),28(B)	51
l = 5	$A_{55}B_{92}$	9.5	10.5	24(B)	36(B)	4(B)	55(A),28(B)	41
Stoichiometric								
l = 2	$A_{13}B_{16}$	5.1	5.5	-	12(B)	12(A)	1(A),4(B)	41
l = 3	$A_{19}B_{16}$	5.5	5.9	-	6(A)	12(A),12(B)	1(A),4(B)	17
l = 4	$A_{43}B_{44}$	7.7	8.4	-	12(A),12(B)	12(A),16(B)	19(A),16(B)	28
l = 5	$A_{69}B_{74}$	9.3	9.9	-	6(A),18(B)	28(A),11(B)	35(A),45(B)	17

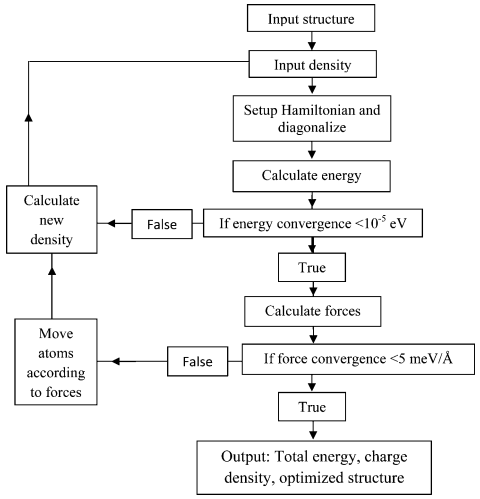

Figure 2. Flowchart of the electronic structure calculation.

In order to understand the stability of NCs as well as surfaces quantitatively, the formation energy was calculated by the formula

$$\Delta H_f = \frac{1}{m+n}[E(A_mB_nHc_pHa_q) - mE(A) - nE(B) - pE(Hc) - qE(Ha) - m\mu_A - n\mu_B]$$

Here, $E(A_mB_nHc_pHa_q)$ is the total energy of the NC or surface consisting of m number of element A, n number of element B, and p and q numbers of the two types of pseudohydrogen atoms, respectively, while $E(A)$ and $E(B)$ are the energies of the elements A and B in their most stable bulk structure. $E(Hc)$ and $E(Ha)$ have been evaluated considering a binary molecule formed by the pseudohydrogens, respectively. As these molecules have different electron counts, we got different energies for $E(Hc)$ and $E(Ha)$. We have considered the orthorhombic structure for Ga,[33] rhombohedral structure for As,[34] and hexagonal structure for both Cd[35] and Se[36] at their experimental lattice constants to evaluate the energies entering

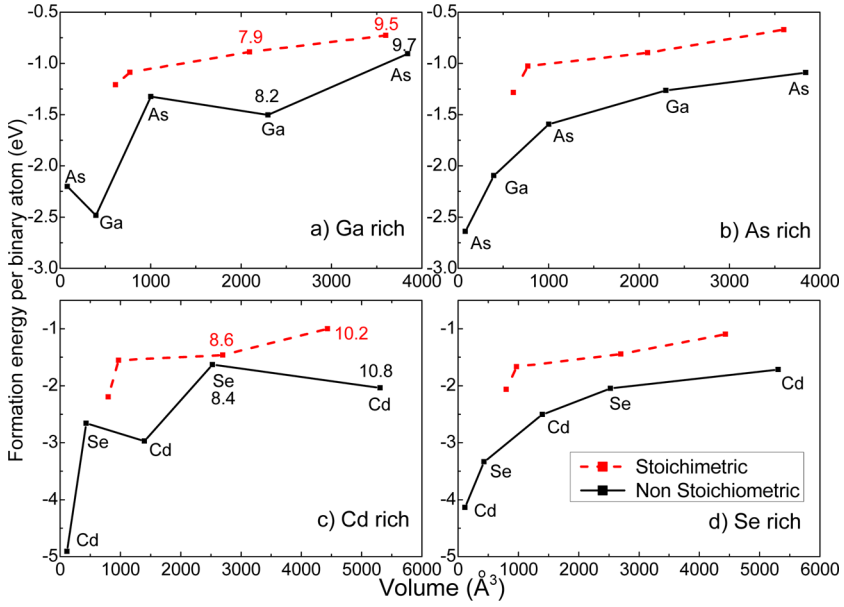

Figure 3. Variation of the formation energy per atom for the passivated NCs of GaAs and CdSe as a function of volume for the nonstoichiometric and stoichiometric NCs under cation-rich (panels a and c) and anion-rich (panels b and d) conditions. Radii of two largest, relaxed NCs have been shown inside panels a and c. Ga and Se atoms lie at the center of GaAs and CdSe NCs, respectively. The type of atom that forms the outermost layer in the case of the nonstoichiometric NCs has been indicated. (The computed points have been indicated with symbols that have been joined by lines to serve as guides to the eye.).

dx.doi.org/10.1021/jp401798y | J. Phys. Chem. C 2013, 117, 21981−21987

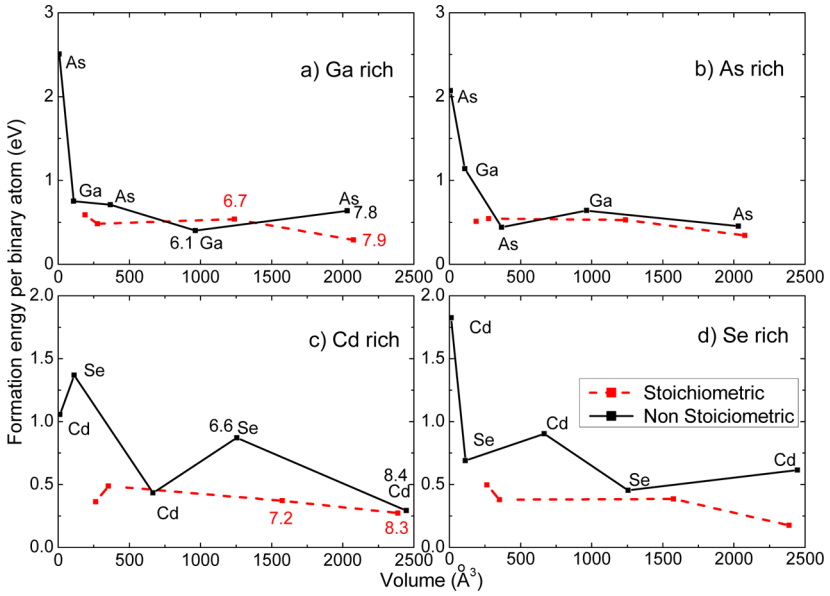

Figure 4. Variation of the formation energy per atom for the unpassivated binary NCs of GaAs and CdSe as a function of volume for the nonstoichiometric and stoichiometric crystals under cation-rich (panels a and c) and anion-rich (panels b and d) conditions. Radii of the two largest, relaxed NCs have been shown inside panels a and c. Ga and Se atoms lie at the center of GaAs and CdSe NCs, respectively. The type of atom that forms the outermost layer in the case of the nonstoichiometric NCs has been indicated. (The computed points have been indicated with symbols that have been joined by lines to serve as guides to the eye.).

the expression for the formation energy. The chemical potentials μ_A and μ_B are determined by the criterion for stability of the bulk solids.

RESULTS AND DISCUSSION

The underlying tetrahedral coordination of the bulk lattice was preserved while constructing the NCs. This has been observed in experiments[37] that probe the local structure. Further, the bond lengths/lattice parameters have been found to be close to the bulk values.[4,38,39] The passivated NCs have been found to capture this effect and do not show significant reconstructions.[27] They observed a reduction in bond length of only ∼1% from their bulk values at the surface of passivated NCs. The candidates chosen for our analysis have equal number of anions and cations in their bulk limit, and one of the motivations was to examine whether this remains to be the case even in the nano regime. Two limiting scenarios of nonstoichiometric and stoichiometric NCs were considered as discussed earlier. To compare the relative stability of different structures, we calculated the formation energies per atom in each case. While the oscillatory behavior in the relative stability for wurtzite versus zincblende structures have been studied in terms of cohesive energy[40] under relaxations of surface atoms only, we carried out complete structural optimization at each volume in order to find the ground state structure and energy. These quantities were computed for limiting values of the chemical potentials, both cation rich as well as anion rich. This was done to examine whether cation-rich conditions would favor a cation-rich surface. In our calculation, we have studied both the experimental limits of excess amount of cations and anions left in the solution.

In order to examine the limiting case of a surface of a NC we consider the nonpolar (110) as well as the polar (100) and (111) surfaces of CdSe in the zinc-blende structure. Details of surface calculations have been mentioned in the Computational Method section. The surface atoms were passivated with pseudohydrogens in each case, and the formation energy of each surface was calculated both with and without the passivating ligands.

The formation energies per atom for passivated NCs of CdSe as well as GaAs are plotted in Figure 3 (Figure 3a,c for cation-rich and Figure 3b,d for anion-rich conditions) as a function of volume. The computed data points have been indicated with symbols, and they have been joined with lines to serve as guides to the eye. Black points with solid lines and red points with dashed lines correspond to the values of formation energy as a function of volume of the NCs for nonstoichiometric and stoichiometric NCs, respectively. In both limits, the cation-rich as well as the anion-rich, one finds that the nonstoichiometric NCs are favored over the stoichiometric ones. As the crystal size increases, the formation energies tend to become less negative. As a consequence of our definition of formation energy, one would expect the value to be zero at the infinite-sized limit where the bulk semiconductor is formed. These results suggest that as the crystal grows, one can have large deviations from the ideal stoichiometry of the bulk with several configurations Cd_nSe_m or Ga_nAs_m being realizable. Two very different systems that were chosen for the study show very similar trends, reinforcing our idea about the generality of these results. Again, the choice of the central atom, as we have chosen Se and Ga as the central atom for CdSe and GaAs NCs, respectively, does not change the trend of our result. The other limit that we consider is that of unpassivated NCs. Surprisingly, one finds that the stoichiometric NCs (as indicated by red points with dashed lines) are the ones favored in almost the entire size regime (Figure 4a−d) that we have studied. There are a few instances when the cation/anion terminated nonstoichiometric NCs have similar or lower formation energy, but the trend seems to indicate stoichiometric NCs are more favorable in the absence of any passivant. The positive value of the formation energy of unpassivated NC suggests that they are unstable. However, the stability could be modified by the

dx.doi.org/10.1021/jp401798y | J. Phys. Chem. C 2013, 117, 21981−21987

presence of solvents, other ions present in the solution and other effects which have not been considered here. This comparison definitely indicates the role being played by passivants. At this juncture we have compared these two limiting cases as the effect of two competing interactions. One is in between cations and passivants and another is in between cations and anions as shown in the schematic diagram Figure 5.

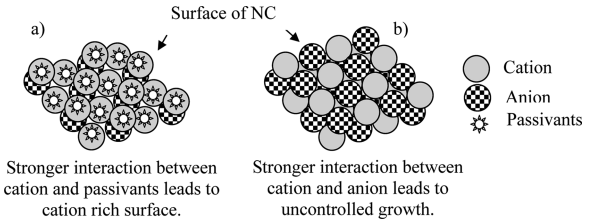

Figure 5. (a) If the interaction strength between cation and passivant is stronger than the interaction strength between cation and anion, a cation rich surface is favored. (b) Stronger interaction between cation and anion leads to an uncontrolled growth of NC.

While the stronger value of the former interaction leads to a cation rich surface (Figure 5a), higher values of the latter interaction leads to an uncontrolled growth of NCs (Figure 5b). The question we then went on to ask was what was it about the passivant that allowed the highly nonstoichiometric crystals to be favored. One way to examine this is to plot the orbital projected partial density of states for the surface as well as the fully coordinated cations/anions. This has been plotted for an l = 4, passivated, nonstoichiometric NC of CdSe in Figure 6. In panel a, the Se p partial density of states has been

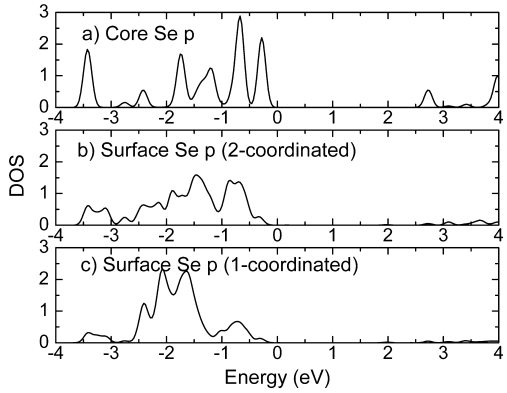

Figure 6. The Se p projected partial density of states (l = 4, nonstoichiometric, and passivated NC) for a Se atom at (a) the core as well as at the surface having (b) double and (c) single coordination with Cd atoms. The zero of energy corresponds to the valence band maximum.

plotted for the Se atom at the core. Zero in these figures represents the valence band maximum. At the surface, one has Se atoms with different coordination, and one finds that the singly coordinated Se atoms have their centroid of the partial density of states deeper (Figure 6c) than the 2-fold coordinated Se atom at the surface (Figure 6b). It should be noted that although we say 2-fold coordinated, we mean 2-fold coordinated with Cd atoms ,while the other two bonds are formed with pseudohydrogens. The change in the centroid of the Se p partial density of states to deeper energies when the numbers of pseudohydrogens/passivant atoms are more suggests strong interaction between the surface atoms and the passivants.

A similar behavior of the partial density of states is seen for the Cd atoms also. The Cd s contribution to the partial density of states in the valence band is plotted in Figure 7a–d for the

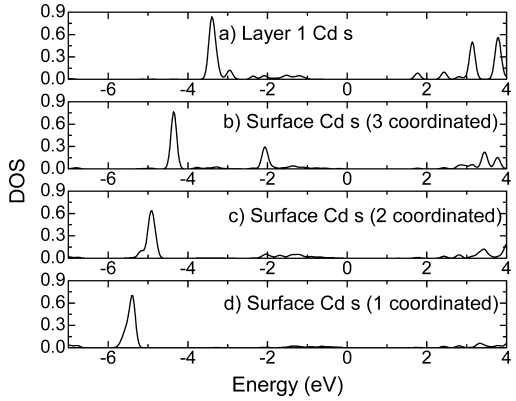

Figure 7. The Cd s projected partial density of states (l = 5, nonstoichiometric, and passivated NC) for a Cd atom (a) in the first layer as well as at the surface having (b) triple, (c) double, and (d) single coordination with the Se atoms. The zero of energy corresponds to the valence band maximum.

case of l = 5, nonstoichiometric, passivated CdSe NC. The Cd s partial density of states associated with the layer next to the core of the NC (layer 1 in our nomenclature) is pushed deeper into the valence band depending on the number of passivant atoms coordinated to the surface Cd atom. This suggests similar strong interaction between the Cd atoms and the passivant.

Although the results plotted in Figure 6 and Figure 7 suggests strong interactions between the surface cations/anions with the passivants, the question we asked is why should this favor the highly nonstoichiometric NCs over the stoichiometric ones. The answer for this is found to be a consequence of the coordination of the surface atoms. The number of atoms with 1-, 2-, 3-, and 4-fold coordination in each of the A_nB_m type of NCs is given in Table 1. Additionally the number of 1-fold and 2-fold coordinated A or B type of atoms in each case is given as a percentage of the total number of atoms. The number of under coordinated atoms seems to be significantly larger for the nonstoichiometric NCs than the stoichiometric ones. As we already pointed out that the under coordinated atoms had the centroid of the partial density of states deeper, indicating a larger energy gain from the interaction of the surface atoms with the passivants, the nonstoichiometric NCs were favored for the passivated case considered.

In order to examine this aspect more carefully, we considered the (100), (110) and the (111) surfaces of CdSe, and calculations for the formation energy were performed both in the presence and absence of passivants. The values are given in Table 2. In every case we find that the passivated surface is stabilized more because of the interaction with the passivants. Further, the interaction with the passivants is found to significantly stabilize the more polar surface (100) and (111). This is consistent with the observations of Soni et al.[22] The coordination of the surface atom is given in each case for the different surfaces one has for zincblende structures in Table 3. The polar surfaces are found to be significantly under-

dx.doi.org/10.1021/jp401798y | J. Phys. Chem. C 2013, 117, 21981–21987

Table 2. Formation Energies for Nonpolar (110) and Polar (100) and (111) Surfaces of CdSe

formation energies per binary atoms for different surfaces of CdSe in eV					
(100)		(110)		(111)	
passivated	unpassivated	passivated	unpassivated	passivated	unpassivated
−0.520	0.166	−0.469	0.068	−0.517	0.070

coordinated, supporting the result of highly nonstoichiometric surfaces being favored.

Table 3. Coordination Number of Surface Atoms for Different Zincblende Surfaces

surface	(100)	(110)	(111)
coordination #	2	3	1,3

The passivants used in the present case are pseudohydrogens that do not have several features that the bulky organic ligands used in experiments have. However, they serve as a guiding principle and suggest that one could use passivants to manipulate the surface stoichiometry. Recent studies[41] have shown that the bulky ligands can be replaced by small inorganic functional groups, and the properties of the NCs remain largely unchanged. Further, the work by Puzder et al.[42] suggests that a significant part of the binding energy of the passivant with the NC surfaces emerges from the end-element attached to the surface atoms. These observations support the use of small atoms, suggesting that the steric effects associated with larger organic ligands may not play such an important role. Currently one has good passivants only for the cations and not the anions. So, by suitably changing the strength of the passivant, one could have a cation-rich surface which would have a stronger efficiency for band edge optical transitions. Soni et al.[21,22] have studied the coverage of CdSe surfaces in experiments using metal oleate passivants. They find using atomic absorption spectroscopy that the Cd coverage at the surface cannot be increased beyond a point inspite of having a high concentration of Cd precursors. So, the present calculations suggest a possible route of how this could be possible.

CONCLUSION

In this work we have shown that passivating ligands introduced during the growth of NCs have a significant role in determining the surface stoichiometry of binary semiconductor NCs. While in the past, their roles had been identified as removing dangling bond states as well as preventing agglomeration of NCs during growth, in this present work we show that the strong interaction between the surface atoms of the NC and the passivant could lead to the passivant determining the surface stoichiometry. Considering two typical examples of binary semiconductors (one, a III−V compound, GaAs, while the other, a II−VI compound, CdSe), we find that highly nonstoichiometric NCs are favored in both cases in the presence of strongly interacting passivants. The results are additionally supported by calculated results on various surfaces of CdSe that were considered.

AUTHOR INFORMATION

Corresponding Author

*Mailing address: S. N. Bose National Centre for Basic Sciences, Block: JD, Sector III, Salt Lake, Kolkata-700098, India. Telephone: +91-33-2335 5706; e-mail: priya@bose.res.in.

Present Address

†Department of Physics, Sacred Heart College Thevara, Kochi - 13, Kerala, India.

Notes

The authors declare no competing financial interest.

ACKNOWLEDGMENTS

The authors thank the Department of Science and Technology (Nano Mission), India and the unit of Nanoscience and Nanotechnology, S. N. Bose Centre. S.D. and R.C. thank the Council of Scientific and Industrial Research, India. We also thank Angshuman Nag for helpful discussions.

REFERENCES

(1) Alivisatos, A. P. Semiconductor Clusters, Nanocrystals, and Quantum Dots. *Science* **1996**, *271*, 933−937.
(2) Alivisatos, A. P. Perspectives on the Physical Chemistry of Semiconductor Nanocrystals. *J. Phys. Chem.* **1996**, *100*, 13226−13239.
(3) Cui, Y.; Wei, Q.; Park, H.; Lieber, C. M. Nanowire Nanosensors for Highly Sensitive and Selective Detection of Biological and Chemical Species. *Science* **2001**, *293*, 1289−1292.
(4) Murray, C. B.; Norris, D. J.; Bawendi, M. G. Synthesis and Characterization of Nearly Monodisperse CdE (E = sulfur, selenium, tellurium) Semiconductor Nanocrystallites. *J. Am. Chem. Soc.* **1993**, *115*, 8706−8715.
(5) Talapin, D. V.; Rogach, A. L.; Kornowski, A.; Haase, M.; Weller, H. Highly Luminescent Monodisperse CdSe and CdSe/ZnS Nanocrystals Synthesized in a Hexadecylamine−Trioctylphosphine Oxide−Trioctylphospine Mixture. *Nano Lett.* **2001**, *1*, 207−211.
(6) Michalet, X.; Pinaud, F. F.; Bentolila, L. A.; Tsay, J. M.; Doose, S.; Li, J. J.; Sundaresan, G.; Wu, A. M.; Gambhir, S. S.; Weiss, S. Quantum Dots for Live Cells, in Vivo Imaging, and Diagnostics. *Science* **2005**, *307*, 538−544.
(7) Tessler, N.; Medvedev, V.; Kazes, M.; Kan, S.; Banin, U. Efficient Near-Infrared Polymer Nanocrystal Light-Emitting Diodes. *Science* **2002**, *295*, 1506−1508.
(8) Chan, T.-L.; Kwak, H.; Eom, J.-H.; Zhang, S. B.; Chelikowsky, J. R. Self-Purification in Si Nanocrystals: An Energetics Study. *Phys. Rev. B* **2010**, *82*, 115421.
(9) Nag, A.; Cherian, R.; Mahadevan, P.; Gopal, A. V.; Hazarika, A.; Mohan, A.; Vengurlekar, A. S.; Sarma, D. D. Size-Dependent Tuning of Mn^{2+} d Emission in Mn^{2+}-Doped CdS Nanocrystals: Bulk vs Surface. *J. Phys. Chem. C* **2010**, *114*, 18323−18329.
(10) Viswanatha, R.; Naveh, D.; Chelikowsky, J. R.; Kronik, L.; Sarma, D. D. Magnetic Properties of Fe/Cu Codoped ZnO Nanocrystals. *J. Phys. Chem. Lett.* **2012**, *3*, 2009−2014.
(11) Alemany, M. M. G.; Tortajada, L.; Huang, X.; Tiago, M. L.; Gallego, L. J.; Chelikowsky, J. R. Role of Dimensionality and Quantum Confinement in p-Type Semiconductor Indium Phosphide Quantum Dots. *Phys. Rev. B* **2008**, *78*, 233101.
(12) Kalyuzhny, G.; Murray, R. W. Ligand Effects on Optical Properties of CdSe Nanocrystals. *J. Phys. Chem. B* **2005**, *109*, 7012−7021.
(13) Bullen, C.; Mulvaney, P. The Effects of Chemisorption on the Luminescence of CdSe Quantum Dots. *Langmuir* **2006**, *22*, 3007−3013.
(14) Nag, A.; Hazarika, A.; Shanavas, K. V.; Sharma, S. M.; Dasgupta, I.; Sarma, D. D. Crystal Structure Engineering by Fine-Tuning the

Surface Energy: The Case of CdE (E = S/Se) Nanocrystals. *J. Phys. Chem. Lett.* **2011**, *2*, 706−712.
(15) Jasieniak, J.; Bullen, C.; van Embden, J.; Mulvaney, P. Phosphine-Free Synthesis of CdSe Nanocrystals. *J. Phys. Chem. B* **2005**, *109*, 20665−20668.
(16) Chen, O.; Yang, Y.; Wang, T.; Wu, H.; Niu, C.; Yang, J.; Cao, Y. C. Surface-Functionalization-Dependent Optical Properties of II−VI Semiconductor Nanocrystals. *J. Am. Chem. Soc.* **2011**, *133*, 17504−17512.
(17) Viswanatha, R.; Amenitsch, H.; Sarma, D. D. Growth Kinetics of ZnO Nanocrystals: A Few Surprises. *J. Am. Chem. Soc.* **2007**, *129*, 4470−4475.
(18) Crespo, P.; Litrán, R.; Rojas, T.; Multigner, M.; De la Fuente, J.; Sánchez-López, J.; Garcia, M.; Hernando, A.; Penadés, S.; Fernández, A. Permanent Magnetism, Magnetic Anisotropy, and Hysteresis of Thiol-Capped Gold Nanoparticles. *Phys. Rev. Lett.* **2004**, *93*, 87204.
(19) Peng, X.; Manna, L.; Yang, W.; Wickham, J.; Scher, E.; Kadavanich, A.; Alivisatos, A. P. Shape Control of CdSe Nanocrystals. *Nature* **2000**, *404*, 59−61.
(20) Akamatsu, K.; Tsuruoka, T.; Nawafune, H. Band Gap Engineering of CdTe Nanocrystals Through Chemical Surface Modification. *J. Am. Chem. Soc.* **2005**, *127*, 1634−1635.
(21) Jasieniak, J.; Mulvaney, P. From Cd-Rich to Se-Rich − The Manipulation of CdSe Nanocrystal Surface Stoichiometry. *J. Am. Chem. Soc.* **2007**, *129*, 2841−2848.
(22) Soni, U.; Sapra, S. The Importance of Surface in Core−Shell Semiconductor Nanocrystals. *J. Phys. Chem. C* **2010**, *114*, 22514−22518.
(23) Yeh, C.-Y.; Lu, Z. W.; Froyen, S.; Zunger, A. Predictions and Systematizations of the Zinc-Blende−Wurtzite Structural Energies in Binary Octet Compounds. *Phys. Rev. B* **1992**, *45*, 12130−12133.
(24) Shiraishi, K. A New Slab Model Approach for Electronic Structure Calculation of Polar Semiconductor Surface. *J. Phys. Soc. Jpn.* **1990**, *59*, 3455−3458.
(25) Hazarika, A.; Layek, A.; De, S.; Nag, A.; Debnath, S.; Mahadevan, P.; Chowdhury, A.; Sarma, D. D. Ultranarrow and Widely Tunable Mn^{2+}-Induced Photoluminescence from Single Mn-Doped Nanocrystals of ZnS-CdS Alloys. *Phys. Rev. Lett.* **2013**, *110*, 267401.
(26) Norberg, N. S.; Dalpian, G. M.; Chelikowsky, J. R.; Gamelin, D. R. Energetic Pinning of Magnetic Impurity Levels in Quantum-Confined Semiconductors. *Nano Lett.* **2006**, *6*, 2887−2892.
(27) Cherian, R.; Mahadevan, P. Size Dependence of Lattice Constants of Semiconductor Nanocrystals. *App. Phys. Lett.* **2008**, *92*, 043130−3.
(28) Kresse, G.; Furthmüller, J. Efficient Iterative Schemes for ab initio Total-Energy Calculations Using a Plane-Wave Basis Set. *Phys. Rev. B* **1996**, *54*, 11169−11186.
(29) Kresse, G.; Furthmüller, J. Efficiency of ab-initio Total Energy Calculations for Metals and Semiconductors Using a Plane-Wave Basis Set. *Comput. Mater. Sci.* **1996**, *6*, 15−50.
(30) Kresse, G.; Joubert, D. From Ultrasoft Pseudopotentials to the Projector Augmented-Wave Method. *Phys. Rev. B* **1999**, *59*, 1758−1775.
(31) Cherian, R.; Mahadevan, P. Bulk and Nanoscale GaN: Role of Ga d States. *Phys. Rev. B* **2007**, *76*, 075205.
(32) Perdew, J. P.; Wang, Y. Accurate and Simple Analytic Representation of the Electron-Gas Correlation Energy. *Phys. Rev. B* **1992**, *45*, 13244−13249.
(33) Sharma, B. D.; Donohue, J. A Refinement of the Crystal Structure of Gallium. *Z. Kristallogr.* **1962**, *177*, 293.
(34) Schiferl, D.; Barrett, C. S. The Crystal Structure of Arsenic at 4.2, 78 and 299 K. *J. App. Cryst.* **1969**, *2*, 30−36.
(35) Jette, E. R.; Foote, F. Precision Determination of Lattice Constants. *J. Chem. Phys.* **1935**, *3*, 605.
(36) Unger, P.; Cherin, P. The Crystal Structure of Trigonal Selenium. *Inorg. Chem.* **1967**, *6*, 1589−1591.
(37) Marcus, M. A.; Brus, L. E.; Murray, C.; Bawendi, M. G.; Prasad, A.; Alivisatos, A. P. EXAFS Studies of Cd Chalcogenide Nanocrystals. *Nanostruct. Mater.* **1992**, *1*, 323−335.
(38) Herron, N.; Calabrese, J. C.; Farneth, W. E.; Wang, Y. Crystal Structure and Optical Properties of $Cd_{32}S_{14}(SC_6H_5)_{36}$. DMF_4, a Cluster with a 15 Angstrom CdS Core. *Science* **1993**, *259*, 1426−1428.
(39) Carter, A. C.; Bouldin, C. E.; Kemner, K. M.; Bell, M. I.; Woicik, J. C.; Majetich, S. A. Surface Structure of Cadmium Selenide Nanocrystallites. *Phys. Rev. B* **1997**, *55*, 13822−13828.
(40) Datta, S.; Kabir, M.; Saha-Dasgupta, T.; Sarma, D. D. First-Principles Study of Structural Stability and Electronic Structure of CdS Nanoclusters. *J. Phys. Chem. C* **2008**, *112*, 8206−8214.
(41) Nag, A.; Chung, D. S.; Dolzhnikov, D. S.; Dimitrijevic, N. M.; Chattopadhyay, S.; Shibata, T.; Talapin, D. V. Effect of Metal Ions on Photoluminescence, Charge Transport, Magnetic and Catalytic Properties of All-Inorganic Colloidal Nanocrystals and Nanocrystal Solids. *J. Am. Chem. Soc.* **2012**, *134*, 13604−13615.
(42) Puzder, A.; Williamson, A. J.; Zaitseva, N.; Galli, G.; Manna, L.; Alivisatos, A. P. The Effect of Organic Ligand Binding on the Growth of CdSe Nanoparticles Probed by Ab Initio Calculations. *Nano Lett.* **2004**, *4*, 2361−2365.